Phytoplankton growth and microzooplankton grazing in high-nutrient, low-chlorophyll waters of the equatorial Pacific: Community and taxon-specific rate assessments from pigment and flow cytometric analyses

Michael R. Landry,[1] Susan L. Brown,[1] Jacques Neveux,[2] Cécile Dupouy,[3] Jean Blanchot,[4] Stephanie Christensen,[1] and Robert R. Bidigare[1]

Received 30 November 2000; revised 22 November 2002; accepted 21 April 2003; published 31 October 2003.

[1] Phytoplankton growth and microzooplankton grazing rates were investigated using the seawater dilution technique during a French Joint Global Ocean Flux Study cruise focusing on grazing processes in the high-nutrient, low-chlorophyll equatorial Pacific at 180° (Etude du Broutage en Zone Equatoriale, October–November, 1996). Raw rate estimates based on spectrofluorometric and high-performance liquid chromatography pigment analyses were typically in close agreement, but most showed substantial imbalances in growth and grazing. Flow cytometric (FCM) analyses were used both as an alternate approach for distinguishing populations and as a means for adjusting pigment-based growth estimates for changes in cellular chlorophyll content and biovolume. Total chlorophyll *a* (Tchl *a*) gave mean community growth rates of 0.76 d^{-1} at 30 m and 0.27 d^{-1} at 60 m. Grazing rates averaged 0.56 and 0.15 d^{-1} at the two depths, respectively, and 69% of phytoplankton growth overall. For the prokaryotic picophytoplankter, *Prochlorococcus* (PRO), rate estimates from dv-chl *a* and FCM cell counts generally indicated balanced growth and grazing and therefore close grazing control by microzooplankton. At the equator, rate estimates from dv-chl *a* averaged 0.6–0.7 d^{-1} at 30 m and 0.25–0.26 at 60 m and were consistent with inferences based on diel pigment variations in the 30–70 m depth range. Phytoplankton production estimates from experimentally determined rates and microscopical assessments of autotrophic carbon at 30 m (mean = 19 mg C m^{-3} d^{-1}) agreed well with contemporaneous measurements by ^{14}C uptake. Diatom growth rate estimates (1.0–1.6 d^{-1}), constrained by contemporaneous measurements of silicate uptake, implied a relatively small biomass (10–45 nmol C L^{-1}) with high rates of turnover and recycling. *INDEX TERMS:* 4231 Oceanography: General: Equatorial oceanography; 4855 Oceanography: Biological and Chemical: Plankton; 4817 Oceanography: Biological and Chemical: Food chains; 4805 Oceanography: Biological and Chemical: Biogeochemical cycles (1615); 4880 Oceanography: Biological and Chemical: Trophodynamics; *KEYWORDS:* protozoa, grazing, growth, pigments, HNLC

Citation: Landry, M. R., S. L. Brown, J. Neveux, C. Dupouy, J. Blanchot, S. Christensen, and R. R. Bidigare, Phytoplankton growth and microzooplankton grazing in high-nutrient, low-chlorophyll waters of the equatorial Pacific: Community and taxon-specific rate assessments from pigment and flow cytometric analyses, *J. Geophys. Res.*, *108*(C12), 8142, doi:10.1029/2000JC000744, 2003.

1. Introduction

[2] Microzooplankton, <200-μm grazers comprised largely of phagotrophic protists, are typically the most effective consumers of phytoplankton in the open oceans [e.g., *Burkill et al.*, 1993; *Verity et al.*, 1993; *Landry et al.*, 1997, 1998]. This follows from their high specific rates of ingestion and growth potential, as well as the dominance of tiny primary producers, unavailable to most large consumers. In open ocean systems generally, and throughout tropical and high-nutrient, low-chlorophyll (HNLC) regions in particular, population abundances of small prey, including bacteria, are thought to be regulated by microzooplankton grazing [*Miller et al.*, 1991; *Landry et al.*, 1998; *Calbet and Landry*, 1999; *Pitchford and Brindley*, 1999]. In the equatorial Pacific, for instance, protistan control of picoplankton and nanoplankton is integral to the explanation of the HNLC condition of relatively low and constant concen-

[1]Department of Oceanography, University of Hawaii at Manoa, Honolulu, Hawaii, USA.
[2]Observatoire Océanologique de Banyuls (CNRS-UPMC), Laboratoire Arago (UMR 7621), Banyuls sur Mer, France.
[3]Laboratoire d'Océanographie Dynamique et de Climatologie (CNRS-IRD-UPMC), UMR 7617, UPMC, Paris, France.
[4]Station Biologique de Roscoff, Institut de Recherche pour le Développement, Roscoff, France.

0148-0227/03/2000JC000744$09.00

trations of fast growing phytoplankton [e.g., *Cullen et al.*, 1992; *Frost and Franzen*, 1992; *Price et al.*, 1994; *Landry et al.*, 1997, 2000b]. As a consequence, changing levels of iron availability are reflected principally in the fluctuations of larger taxa such as diatoms [e.g., *Morel et al.*, 1991; *Bidigare and Ondrusek*, 1996; *Coale et al.*, 1996; *Landry et al.*, 2000a].

[3] Cell cycle analyses and inferences from diel cycles in picophytoplankton abundances provide strong support for rapid growth and control processes in HNLC systems [*Vaulot et al.*, 1995; *André et al.*, 1999; *Vaulot and Marie*, 1999; *Neveux et al.*, 2003]. However, they do not directly measure grazing or distinguish between grazing and other loss mechanisms (e.g., viral lysis). On the other hand, techniques that should better demonstrate a balance between growth and grazing processes, such as seawater dilution [*Landry and Hassett*, 1982], have often yielded equivocal results [*Landry et al.*, 1995b, 2000b; *Latasa et al.*, 1997]. As part of a French Joint Global Ocean Flux Study (JGOFS) cruise (Etude du Broutage en Zone Equatoriale (EBENE), October–November 1996) which focused on grazing processes in HNLC waters [*Le Borgne and Landry*, 2003], we attempted to evaluate more carefully the growth and grazing dynamics of picoplankton using both flow cytometric and taxon-specific pigment indices. These complementary analyses also allowed us to adjust growth rate inferences from spectrofluorometric and high-performance liquid chromatography (HPLC) pigment analyses for changes in cellular pigment content and biovolume, and thus to better resolve the dynamics of growth and grazing at the community level.

2. Materials and Methods

[4] Mean daily rates of phytoplankton growth and microzooplankton grazing were estimated according to the dilution protocols of *Landry et al.* [1998] at two stations (3°S and 0°, 180°) on the EBENE cruise. These 24-hour incubation experiments began at 2200 on 31 October at 3°S and at 1300 (4 November), 2200 (6 November) and 2200 (8 November) at the equator station. For each time period, one experiment was conducted with water collected from the mixed layer at 30 m, and one was conducted with water from 60-m depth. Rate estimates for the 8 experiments were determined both for the phytoplankton community as a whole and for specific populations based on pigment determinations by spectrofluorometry (SpFl) and high-performance liquid chromatography (HPLC) and cell abundances from flow cytometry (FCM).

2.1. Experimental Set Up

[5] Experimental seawater was collected in 10-L, Teflon-lined Go-Flo bottles on Kevlar wire, closed by Teflon-coated messengers. The bottles were lowered in pairs to 30 and 60 m, and the contents of several bottles for each depth were mixed gently in clean 20-L polycarbonate carboys. Filtered water was obtained by direct gravity flow from CTD rosette bottles through an in-line filter capsule (Gelman Criticap 100, 0.2-μm pore size, presoaked for 1 hour in 10% HCl) to a clean polycarbonate carboy. All experimental containers and transfer tubing (silicone) were trace metal cleaned before the cruise [*Fitzwater et al.*, 1982] and rinsed between uses with 10% trace metal grade HCl-Milli-Q water and freshly collected seawater (3 times). Plastic gloves were worn during all phases of experimental setup, subsampling and cleaning.

[6] For each experiment (depth), ten 2.2-L polycarbonate bottles were used to establish a nutrient-enriched dilution series consisting of replicated bottles with 22, 45, 65, 86 and 100% natural (unfiltered) seawater. The filtered water was added first to the experimental bottles in measured amounts; then the bottles were gently filled and mixed with unfiltered seawater from the same depth. Aliquots of a nutrient mixture (0.5 μM ammonium, 0.03 μM phosphate and 1.0 nM $FeSO_4$) and fluorescently labeled bacteria (FLB, ~3,700 cells mL^{-1} final concentration) were also added to dilution treatments and mixed thoroughly during the filling procedure [*Landry et al.*, 1995b]. FLB were prepared from carbon-starved cultures of *Vibrio damsella* (1.1-μm diameter) according to the procedures of *Sherr et al.* [1987]. Five more bottles were filled with whole seawater without nutrient enrichment. Three of these were used for initial sampling (pigments, cytometry and microscopy), and the final two were incubated as natural seawater controls. One additional bottle was filled with filtered seawater and run as a blank control. All bottles were tightly capped and incubated for 24 hours in seawater-cooled shipboard incubators constructed of light blue (color 2069) or dark blue (color 2424) Plexiglas and screened with neutral density fabric. The light levels in the boxes were 15 and 3% of surface PAR, approximately the light conditions at the 30- and 60-m sampling depths.

2.2. Spectrofluorometric Pigments

[7] Shipboard analyses of pigments were based on the spectrofluorometric method of *Neveux and Lantoine* [1993]. Seawater samples (500 mL) were filtered onto 47-mm Whatman GF/F glass fiber filters and ground in 5.4 mL of 100% acetone (90% with retained water in the filter) with the fresh broken end of a glass rod. After a 12-hour extraction in the dark at 4°C, the samples were centrifuged and analyzed on a Hitachi F4500 spectrofluorometer in the ratio mode. Slit widths were set at 5 and 10 nm for excitation and emission, respectively. Fluorescence emission spectra were acquired for each of 31 excitation wavelengths (3-nm increments from 390 to 480 nm). Emission spectra were recorded at 4-nm intervals from 615 to 715 nm, yielding 26 data points for each spectrum. Pigment concentrations were estimated from the resulting 806 data points (31 × 26) according to least squares approximation [*Neveux and Lantoine*, 1993].

2.3. HPLC Pigments

[8] Seawater samples (~1.6 L) for pigment analyses were concentrated onto 25-mm Whatman GF/F glass fiber filters. The filters were wrapped in aluminum foil, frozen in liquid nitrogen and stored at −85°C until analysis. Pigments were extracted in 3 mL of 100% acetone in the dark at 0°C for 24 hours, following disruption of the cells by sonication. Canthaxanthin (50 μL in acetone) was added as an internal standard to all samples. Prior to analysis, the pigment extracts were vortexed and centrifuged to remove cellular debris.

[9] Subsamples of 200 μL of a mixture of 1.0 mL pigment extract and 0.3 mL H_2O were injected into a Varian

9012 HPLC system equipped with Varian 9300 autosampler, a Timberline column heater (26°C), and Spherisorb 5-μm ODS2 analytical column (4.6 × 250 mm) and corresponding guard cartridge. Pigments were detected with a ThermoSeparation Products UV2000 absorbance (436 nm) detector and analyzed according to *Andersen et al.* [1998]. Separations followed a modified ternary solvent protocol [*Wright et al.*, 1991], with eluent A = 80:20 mixture of methanol:0.5 M ammonium acetate with 0.01% 2,6-di-tert-butyl-p-cresol; eluent B = 85:15 mixture of acetonitrile:-water; and eluent C = ethyl acetate. The linear gradient was 0′ (90%A, 10%B), 1′ (100%B), 11′ (78%B, 22%C), 27.5′ (10%B, 90%C), 29′ (100%B), and 30′ (100%B). Peak identifications were made by comparing the retention times of eluting peaks with those of pure standards and extracts prepared from algal cultures of known pigment composition [*Bidigare*, 1991; *Latasa et al.*, 1996].

2.4. Flow Cytometric (FCM) Analyses

[10] FCM samples (1 mL) were preserved with 0.5% paraformaldehyde (final concentration), frozen in liquid nitrogen and stored at −85°C until analysis. Frozen samples were thawed and stained in the dark with Hoechst 33342 (1 μg mL^{-1}) for 1 hour prior to analysis [*Monger and Landry*, 1993]. Subsamples (100 μl) were enumerated with a Coulter EPICS 753 flow cytometer equipped with dual 5W argon lasers, MSDS II automatic sampling, a Biosense flow cell and CICERO Cytomation software. The dual lasers were aligned colinearily with the first tuned to the UV range at 225 mW to excite Hoechst-stained DNA. The second was tuned to 488 nm at 1.0 W to elicit red autofluorescence of chlorophyll-containing cells. Forward angle light scatter (FALS), right angle light scatter (RALS) and four fluorescence signals were collected for each cell, stored in list mode files, and analyzed using CYTOPC software [*Vaulot*, 1989]. Light scattering and fluorescence signals were normalized to standard beads (0.57 and 0.98-μm YG Fluoresbrite microspheres for visible excitation and 0.46-μm UV excitable beads, Polysciences) added to each sample. Where presented as biomass, FCM cell counts of prokaryotic autotrophs (PRO and SYN) were converted to cellular carbon using factors of 35 and 100 fg C $cell^{-1}$ for PRO and SYN, respectively [*Garrison et al.*, 2000; *Landry and Kirchman*, 2002].

[11] In addition to analysis of preserved samples as described above, most of the experiments (excluding those on 4 November) were also enumerated live on shipboard by the method of *Blanchot and Rodier* [1996]. These analyses were performed using a Becton-Dickinson FACScan cytometer with 15 mW argon laser at 488 nm. The cytometer was housed in a dark, temperature regulated room, and GF/F filtered seawater from 1000 m was used as the sheath fluid. Volumes of approximately 120 μL were counted, with the flow rate determined before each sample set using a known concentration of beads. List mode files were analyzed with Lysis II software.

2.5. Microscopical Analyses

[12] Autotrophic and heterotrophic eukaryotic protists >1.5 μm in linear dimension were enumerated from 50-mL samples preserved with 0.5% paraformaldehyde and stained with 25 μL of 0.033% (w/v) proflavin. The samples were concentrated on 0.6-μm, 25-μm black polycarbonate membrane filters and stained briefly with DAPI (10 μg mL^{-1}) in the final stages of filtration [*Sherr and Sherr*, 1993]. Filters were mounted on glass slides with a drop of immersion oil and frozen at −70°C. Thawed slides were analyzed with a color image analysis system consisting of a Zeiss Standard epifluoresence microscope with a 100 W power supply, and C-mounted Zeiss 3 CCD video camera and ZVS-3C75DE processor. The images were processed using Zeiss Image Pro Plus software to facilitate counting and sizing. Cellular carbon contents (pg C) of autotrophic and heterotrophic taxa were estimated from cellular biovolumes (BV, μm^3) following the modified *Strathmann* [1967] equations of *Eppley et al.* [1970]: $\log_{10}C = 0.94 * \log_{10}BV - 0.60$ for nondiatoms and $\log_{10}C = 0.76 * \log_{10}BV - 0.352$ for diatoms [*Garrison et al.*, 2000].

[13] For experiments conducted on 31 October and 4 November, biomass estimates from slides as described above were augmented with additional analyses from hydrographic sampling from the same depths and only slightly different in time [*Brown et al.*, 2003]. These samples, including additional 50-mL samples (as above) and 250-mL subsamples preserved according to *Sherr and Sherr* [1993] and filtered onto 8-μm filters, allowed better estimation of the biomass of relatively rare large taxa than could be achieved with the smaller volume slides. To estimate more robustly the biomass of autotrophic eukaryotes (C_{euk}) on 6 and 8 November, we used the initial values of mv-chl *a* for those experiments (Table 2) and the mean ratios of C_{euk}:mv-chl *a* determined for the 30 and 60-m depths on the previous dates.

2.6. Rate Estimates

[14] Initial pigment concentrations and FCM population abundances ($C_{i,o}$) were determined for each dilution treatment from measured concentrations in the unfiltered seawater and the proportion of unfiltered (D_i) water in the treatment. Final concentrations ($C_{i,t}$) were measured in each bottle at the end of the 24-hour incubations. Daily net rates of change (d^{-1}) were determined as $k_i = \ln(C_{i,t}/C_{i,o})$. From these data, we derived daily rate estimates of specific mortality due to microzooplankton grazing (m, d^{-1}) from the slopes of linear regressions of k_i against D_i (n = 10 nutrient amended bottles). Parameter-specific estimates of phytoplankton growth rate (μ, d^{-1}) were then computed as the sum of grazing mortality (m) and mean net growth rate (k_o) in the unamended seawater treatments (i.e., $\mu = k_o + m$).

[15] Mortality rate estimates from the above calculations were assumed to be unaffected by changes in phytoplankton physiological condition during the experimental incubations [*Landry*, 1993]. However, growth rate estimates could either be exaggerated or understated by physiological adjustments. We attempted to correct for such effects using red fluorescence from the FCM analyses as an indicator of cell chl *a* content and FALS as a relative measure of cellular biovolume. Cell biovolumes of *Prochlorococcus* and *Synechococcus* have been determined to vary with $FALS^{0.55}$ [*DuRand*, 1995; *Binder et al.*, 1996]. Given the relatively linear relationship between FALS and Mie scattering cross section for cells in the size range of *Synechococcus* to *Nannochloris* (8 μm) [*DuRand and Olson*, 1996], we assumed that the same exponent would be applicable to

small photosynthetic eukaryotes (PEUK), as a reasonable first approximation. On the basis of microscopical analyses of near-surface samples from the two experimental stations, an average of 67% of the eukaryotic phytoplankton were less than 2 μm in their longest linear dimension, 87% were <3 μm, and <3% exceeded 5 μm in length. In theory, scattering per cell biovolume decreases with increasing cell size [*Morel*, 1991; *Shalapyonok et al.*, 2001]. The exponent in the BV to FALS relationship therefore increases, and a constant exponent will tend to underestimate the BV changes of larger cells.

[16] To make biovolume adjustments for rates determined from FCM cell counts, the computed growth estimates (μ_o) were expressed in terms of two components, the growth rates (μ_o') of cells in balanced growth and the growth (g_{BV}) associated with unbalanced changes in mean cell biovolume (i.e., $\mu_o = \mu_o' - g_{BV}$). Increases in cell size need to be added to observed changes in cell abundances to determine true biovolume-balanced growth rates. Accordingly, for each of the FCM-distinguished populations (PRO, SYN and PEUK), biovolume-adjusted growth rate estimates (μ_o') were determined as:

$$\mu_o' = \mu_o + \ln\left[(FALS_f/FALS_i)^{0.55}\right]$$

where the initial and final FALS estimates are denoted by subscripts "i" and "f", respectively, and experiment duration is understood to be one day. Similarly, calculated chlorophyll-based growth rate estimates were adjusted for changes in cellular pigment density (CPD), a chl:C proxy, computed from bead-normalized determinations of red fluorescence (RF) and FALS as: $CPD = RF/FALS^{0.55}$. As above, adjusted rates (μ_o') were computed for each of the FCM populations as

$$\mu_o' = \mu_o - \ln(CPD_f/CPD_i)$$

This calculation has the effect of removing from the raw pigment-based estimates any changes in pigment concentration that are disproportionate to the net rates of change of cellular biovolume (i.e., biomass). The CPD adjustment is straightforward for divinyl chlorophyll *a* (dv-chl *a*), which is unambiguously associated with *Prochlorococcus* cells. For monovinyl and total chl *a* (mv-chl *a* and Tchl *a*), we weighted PRO, SYN and PEUK populations according to their respective contributions to mean total red fluorescence during the incubations.

[17] Instantaneous rates of phytoplankton community growth (adjusted as above) and grazing mortality were used to compute phytoplankton biomass production (PP, μg C L^{-1} d^{-1}) and grazing losses (G, μg C L^{-1} d^{-1}) according to the following equations:

$$PP = \mu_o' * C_m$$

$$G = m * C_m$$

$$\text{and } C_m = C_{phyto}\left[e^{(\mu - m)t} - 1\right]/(\mu_o' - m)t$$

where C_m is the geometric mean concentration of phytoplankton carbon during the experiment and C_{phyto} is the initial phytoplankton carbon biomass determined from microscopical and FCM analyses [*Landry and Hassett*, 1982; *Landry et al.*, 2000b].

Table 1. Abbreviations and Taxonomic Affinities for Experimental Rate Determinations in the Present Study[a]

Parameter	Abbreviation	Phytoplankton Taxa
	Pigments	
Total chlorophyll *a*	Tchl *a*	All phytoplankton
Chlorophyll *b*	chl *b*	PRO[b]
Divinyl chlorophyll *a*	dv-chl *a*	PRO[b]
Monovinyl chlorophyll *a*	mv-chl *a*	DIAT, DINO, PELAGO, PRYM, SYN
α-Carotene	αCAR	PRO[b]
β-Carotene	βCAR	DIAT, DINO, PELAGO, PRYMN, SYN
19′-Butanoyloxyfucoxanthin	BUT	PELAGO,[b] PRYMN
Diadinoxanthin	DDX	DIAT, DINO, PELAGO, PRYMN
Fucoxanthin	FUCO	DIAT,[b] PELAGO, PRYMN
19′-Hexanoyloxyfucoxanthin	HEX	PRYMN,[b] PELAGO
Peridinin	PER	
Zeaxanthin	ZEAX	PRO,[b] SYN[b]
	Flow Cytometry	
Prochlorococcus spp.	PRO	PRO[b]
Synechococcus spp.	SYN	SYN[b]
Picoeukaryotic algae	PEUK	mixed PELAGO, PRYMN

[a]Pigment taxa assignments based on *Jeffrey and Vesk* [1997], as well as pigment size fractionation and other accessory pigment information as described in text. PRO, *Prochlorococcus*; SYN, *Synechococcus*; DIAT, diatoms; DINO, dinoflagellates; PRYMN, prymnesiophytes; and PELAGO, pelagophytes.

[b]Taxa assumed to be dominant contributors to the measured parameter.

3. Results

3.1. Parameter Definitions and Taxonomic Assignments

[18] Table 1 lists the parameters measured in the present study and their assignments to major phytoplankton taxa. For flow cytometric (FCM) counts of prokaryotic autotrophs, *Prochlorococcus* (PRO) and *Synechococcus* (SYN), these assignments were straightforward. FCM counts of photosynthetic eukaryotes (PEUK), however, comprised a mixed assemblage of taxa, dominated numerically by cells <3 μm in diameter. For pigments, taxonomic assignments were based on known pigment compositions of the various groups [*Jeffrey and Vesk*, 1997], as well as relevant ancillary evidence from the study site and other equatorial studies. For example, low standing stocks of chlorophytes, prasinophytes, and cryptophytes were indicated by negligible concentrations of their accessory pigments (lutein, prasinoxanthin, and alloxanthin). We thus ignored the contributions of these taxa to chl *b*, α-carotene (α-CAR) and zeaxanthin (ZEAX). These later three pigments were further assumed to reside mostly in the prokaryotic picoplankton based on size fraction analysis and experimental results from the IronEx II study [*Landry et al.*, 2000b; *Latasa and Bidigare*, 1998], although the source of chl *b* remains controversial [*Neveux et al.*, 2003].

[19] Mv-chl *a*, β-carotene (β-CAR) and diadinoxanthin (DDX) are broadly distributed among eukaryotic algae. Among the pigments with stronger group affinities, the overlap in dominant accessory pigments between prymnesiophytes (PRYMN) and pelagophytes (PELAGO) makes

Table 2. Summary of Dilution Experimental Results for Samples Collected at 30 and 60 m on the EBENE Cruise[a]

	30 m			60 m		
Parameter	C_0	μ, d^{-1}	m, d^{-1}	C_0	μ, d^{-1}	m, d^{-1}
			Spectrofluorometric Pigments			
Tchl *a*	279 (39)	1.00 (0.22)	0.55 (0.17)	307 (43)	0.54 (0.07)	0.11 (0.05)
Mv-chl *a*	160 (33)	1.17 (0.22)	0.51 (0.20)	175 (30)	0.60 (0.02)	0.08 (0.09)
Dv-chl *a*	119 (10)	0.74 (0.26)	0.65 (0.20)	133 (17)	0.45 (0.19)	0.15 (0.06)
Mv-chl *b*	75 (4)	0.61 (0.29)	0.40 (0.18)	87 (8)	0.31 (0.12)	0.06 (0.05)
Chl *c*	36 (7)	1.06 (0.22)	0.50 (0.28)	42 (9)	0.45 (0.05)	0.07 (0.08)
			HPLC Pigments			
Tchl *a*	271 (27)	1.02 (0.24)	0.57 (0.20)	330 (40)	0.59 (0.19)	0.18 (0.13)
Mv-chl *a*	171 (29)	1.19 (0.23)	0.53 (0.26)	205 (35)	0.64 (0.12)	0.14 (0.12)
Dv-chl *a*	100 (8)	0.65 (0.22)	0.71 (0.08)	125 (13)	0.52 (0.31)	0.25 (0.16)
Chl *b*	53 (1)	0.74 (0.24)	0.71 (0.29)	76 (3)	0.53 (0.18)	0.34 (0.23)
α-CAR	22 (2)	1.08 (0.22)	0.89 (0.07)	27 (3)	0.75 (0.28)	0.42 (0.15)
β-CAR	5 (2)	1.41 (0.06)	0.57 (0.19)	5 (1)	0.94 (0.06)	0.27 (0.09)
BUT	34 (10)	1.20 (0.38)	0.53 (0.41)	49 (17)	0.47 (0.23)	0.19 (0.10)
DDX	23 (9)	0.64 (0.47)	0.49 (0.34)	14 (2)	0.64 (0.05)	0.28 (0.08)
FUCO	14 (5)	1.91 (0.19)	0.50 (0.21)	17 (7)	0.91 (0.09)	0.22 (0.14)
HEX	103 (6)	1.10 (0.32)	0.53 (0.43)	129 (17)	0.30 (0.18)	0.15 (0.08)
PER	8 (2)	0.60 (0.41)	0.31 (0.20)	10 (2)	0.50 (0.19)	0.37 (0.17)
ZEAX	110 (11)	0.66 (0.24)	0.48 (0.10)	87 (7)	0.50 (0.27)	0.28 (0.17)
			Flow Cytometry			
PRO-pres	176 (51)	0.31 (0.18)	0.61 (0.15)	140 (36)	0.27 (0.15)	0.37 (0.10)
PRO-live	201 (20)	0.35 (0.11)	0.81 (0.16)	188 (17)	0.13 (0.08)	0.33 (0.12)
SYN-pres	15 (6)	0.57 (0.17)	0.43 (0.08)	11 (3)	0.26 (0.22)	0.37 (0.12)
SYN-live	15 (4)	0.62 (0.16)	0.38 (0.14)	13 (2)	0.14 (0.08)	0.34 (0.15)
PEUK-pres	6 (1)	0.35 (0.28)	0.55 (0.38)	5 (0.5)	0.27 (0.07)	0.32 (0.11)
FLB	4 (0.6)		0.31 (0.14)	4 (0.6)		0.40 (0.14)

[a] C_0, initial parameter values; ng L^{-1} for spectrofluorometric and HPLC pigment determinations and 10^3 cells mL^{-1} for flow cytometric analyses (preserved and live counted). Rate estimates are for phytoplankton growth (μ, d^{-1}) and microzooplankton grazing (m, d^{-1}). Parentheses enclose standard deviations of the mean estimates; n = 4 except live FCM counts (n = 3).

these groups difficult to separate unambiguously, although 19′-butanoyloxyfucoxanthin (BUT) is most strongly expressed in pelagophytes while 19′-hexanoyloxyfucoxanthin (HEX) is more representative of PRYMN. PRYMN and PELAGO may also contain some fucoxanthin (FUCO), but that was assumed to reside principally in diatoms (DIAT).

3.2. Mean Standing Stocks and Rates

[20] Mean estimates of the standing stocks and experimental rate determinations are given in Table 2 for the various parameters measured from 30- and 60-m samples. Where the pigment-based estimates of standing stocks can be compared directly, the spectrofluorometric and HPLC determinations agreed fairly closely. For comparable values of Tchl *a*, however, spectrofluorometry gave a slightly higher mean ratio of dv-chl *a* to Tchl *a*, 0.43 compared to 0.37 from HPLC. In addition, chl *b* concentrations were a little lower on average for the HPLC determinations. HPLC did not discriminate mv-chl *b* from dv-chl *b* whereas spectrofluorometry indicated that virtually all of the chl *b* in the upper 60 m was the monovinyl type [*Neveux et al.*, 2003]. Spectrofluorometric estimates of chl *c* were similar to the combined values for chl *c1*+2 from HPLC analyses (not shown), but these chl *c* pigments were near the detection limit in the more diluted experimental treatments and unreliable for rate determinations.

[21] For FCM populations, live analyses of PRO abundances averaged about 20% higher than subsequent counts of preserved samples. Half of this difference was due to the absence of live counts for one experiment (4 November), for which the preserved counts were much lower than the other experiments and which contributed most to the higher standard deviations of the preserved counts. The remaining 10% discrepancy may be explained by losses due to preservation and freezing or to population increases in the live samples while they waited one to several hours before analysis. Although these samples were placed in a dark refrigerator to minimize population changes, some net growth may have been inevitable as the experimental setup (late afternoon and evenings) was during the time of synchronized cell division [*Vaulot and Marie*, 1999].

[22] Mean growth rate estimates at 30 m varied from about 0.3 d^{-1} for PRO to 1.9 d^{-1} for FUCO (Table 2). Most, including the Tchl *a* estimate for the composite phytoplankton community (1.0 d^{-1}), were in the range of 0.6 to 1.2 d^{-1}. Growth rate estimates for the 60-m samples were about half of the values for 30 m, ranging from 0.1 to 0.9 d^{-1}. Microzooplankton grazing rates averaged about half of community growth rate estimates at 30 m and 20–30% at 60 m, on the basis of analyses of Tchl *a*. However, the m:μ ratio was highly variable for the different parameters measured, as will be considered further below.

3.3. Rate Estimates from Spectrofluorometric Versus HPLC Pigments

[23] Rate assessments based on the spectrofluorometric and HPLC pigment techniques were generally in close agreement for the chlorophyll *a* pigments. For both 30- and 60-m experiments, for instance, mean rate estimates from the different Tchl *a*, mv-chl *a* and dv-chl *a* analyses

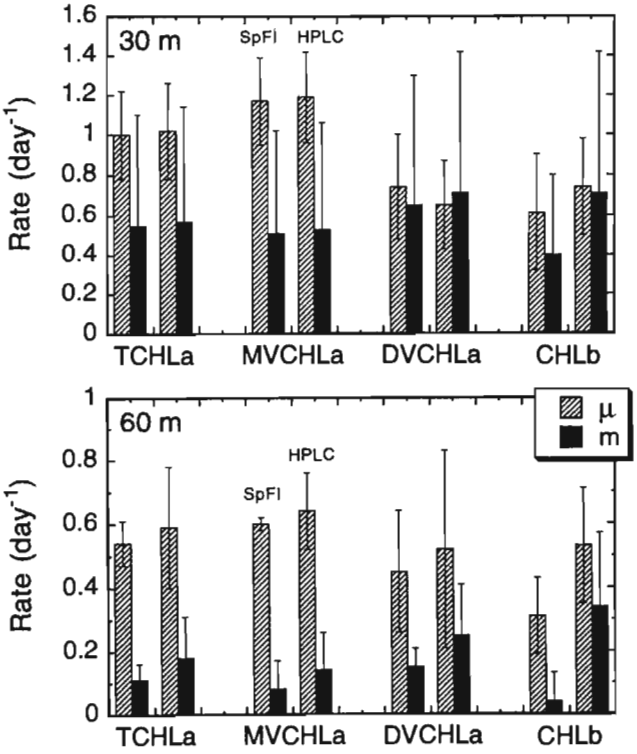

Figure 1. Comparison of mean dilution rate estimates for phytoplankton growth (μ_o) and microzooplankton grazing (g) based on chlorophyll analyses by spectrofluorometry (SpFl) and HPLC. Vertical line denotes one standard deviation (n = 4 experiments with water from 30 or 60 m).

agreed within 0.1 d^{-1} (Figure 1). The largest difference for an individual experiment was ~0.3 d^{-1} (Figure 2). Even when the HPLC determinations gave slightly higher mean rates at 60 m, the magnitudes of the differences between μ and m, and the rate trends (mv-chl > Tchl > dv-chl for μ, and the opposite for m), were similar for the two techniques. Given these opposing trends, dv-chl *a* displayed a m:μ ratio much closer to 1.0 (grazing balance) than mv-chl *a* or Tchl *a*. There was essentially no difference between growth and grazing estimates for dv-chl *a* at 30 m, while the net growth rate differential at 60 m was about 0.3 d^{-1}. Mv-chl *a*, in contrast, gave m:μ grazing ratios <0.5 and net growth differentials (μ-m) > 0.5 d^{-1} at both depths.

[24] In contrast to the chl *a* results, rate estimates from spectrofluorometric and HPLC analyses of chl *b* showed substantial differences (Figure 1). For HPLC measurements, rate estimates for chl *b* were closely linked to those for dv-chl *a*, implying a common source (Table 1). For spectrofluorometric determinations, both μ and m estimates for chl *b* were substantially lower than HLPC rates for chl *b* or spectrofluorometric rates for dv-chl *a*. *Neveux et al.* [2003] discuss alternative explanations for the discrepancy in chl *b* measurements, but the issue remains unresolved.

3.4. Taxon-Specific Rate Estimates

[25] From analyses based on HPLC pigments, substantial rate differences were exhibited among eukaryotic phytoplankton groups as well as between depths (Figure 3). At 30 m, for instance, the grazing rate estimates tended to be similar for the different pigments, clustering around 0.5 d^{-1} except for a slightly lower mean rate (0.3 d^{-1}) for the dinoflagellate pigment, peridinin. However, growth rates were quite variable among groups at 30 m, with rate estimates for pelagophytes (BUT) and prymnesiophytes (HEX) falling between the diatom (FUCO) and dinoflagel-

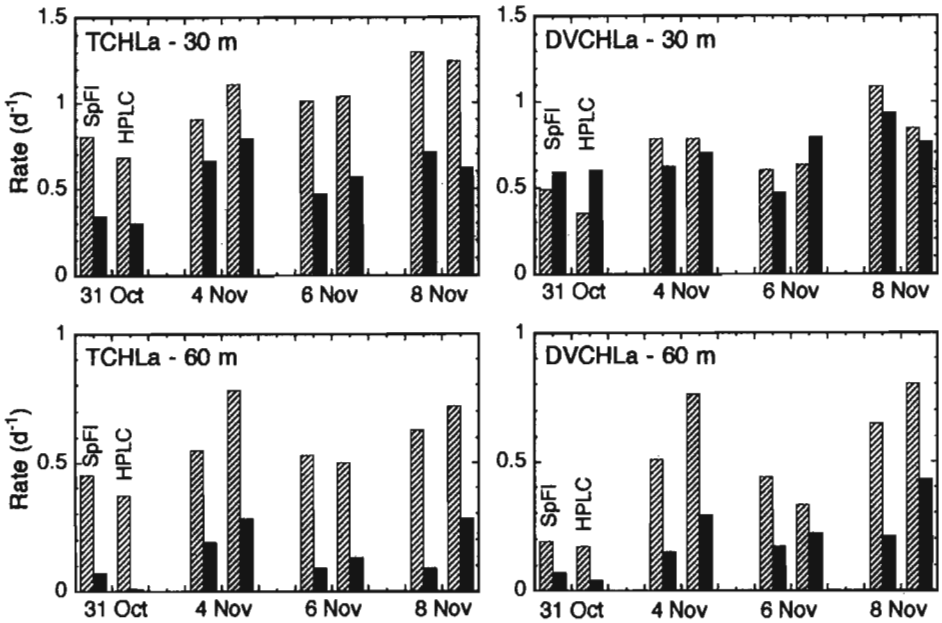

Figure 2. Comparison of chlorophyll-based rate estimates from individual dilution experiments analyzed by spectrofluorometry and HPLC. Hatched histogram = growth rate (μ, d^{-1}). Dark histogram = grazing rate (m, d^{-1}).

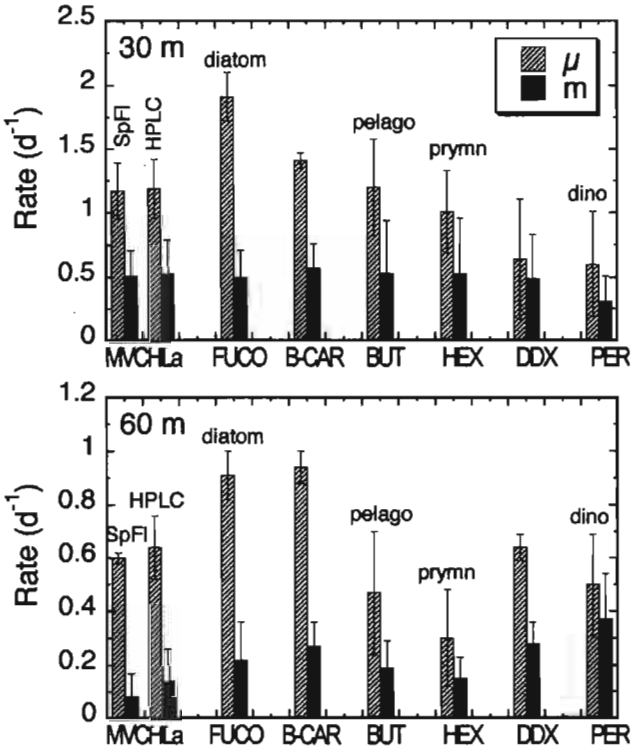

Figure 3. Comparison of mean dilution rate estimates for pigments associated with eukaryotic phytoplankton groups (Table 1). Vertical line denotes one standard deviation (n = 4 experiments with water from 30 and 60 m).

late (PER) extremes and close to the broadly distributed eukaryotic pigments (mv-chl *a*, βCAR and DDX). FUCO also gave the highest group-specific growth rate at 60 m, but the estimates for BUT and HEX were lower than those for the nonspecific pigments. In addition, the grazing rate estimates were more variable at 60 m, with the highest for PER and the lowest for HEX and mv-chl *a*. Somewhat surprisingly, the mean grazing rate determinations for the pigment common to all eukaryotic algae (mv-chl *a*) were lower than those for all groups individually.

[26] Whereas growth rates markedly exceeded grazing estimates for all indices of eukaryotic algae (Figure 3), these rates tended to be more similar for prokaryotes. In the 30-m experiments, for example, most of the growth and grazing estimate for each prokaryote-associated parameter were in the range of one cell doubling d^{-1} (0.6–0.8 d^{-1}) (Figure 4). PRO growth rates from live and preserved FCM analyses were about half that (~0.3 d^{-1}), and estimates for α-CAR were higher (>1.0 d^{-1}; Table 2). Spectrofluorometric determinations of grazing rates from chl *b* and FCM mortality estimates for SYN were also on the low side (~0.4 d^{-1}).

[27] Although some prokaryote growth estimates from individual experiments with 60-m water were consistent with rates of one cell doubling d^{-1} (e.g., dv-chl *a* in Figure 2; also α-CAR and chl *b* from HPLC analyses; Table 2), the mean rate estimates tended to be lower, typically 0.3–0.5 d^{-1} (Figure 4). For PRO and SYN, grazing estimates were similar for live and preserved analyses, but growth rates from the live analyses were ~0.1 d^{-1} lower than those from preserved samples. Neither, however, bore a strong similarity to pigment-based estimates for dv-chl *a* and ZEAX, for which μ substantially exceeded m, while μ < m for FCM determinations.

3.5. FCM-Adjusted Rate Estimates

[28] All populations distinguishable by FCM analyses increased in cellular red fluorescence during all experiments. For PRO, SYN and PEUK cells in the 30-m experiments, the mean instantaneous rates of change (Table 3) were equivalent to daily increases of 20, 66 and 42%, respectively. At 60 m, the fluorescence increases for these populations were 33, 62 and 54% d^{-1}. A tight linear relationship between *Prochlorococcus* population RF and dv-chl *a* (Figure 5), including all initial and final sample analyses from both depths, supports the assumption that the RF changes parallel those of cell chlorophyll content. Our RF measurements were more variable for the total phytoplankton community because large and rare cells were inadequately represented in the small sample sizes. Nonetheless, the relationship between total community RF and Tchl *a* (Figure 5) is also relatively strong and linear, consistent with our assumption.

[29] In all experiments, fluorescence changes for the eukaryotic cells were accompanied by significant increases

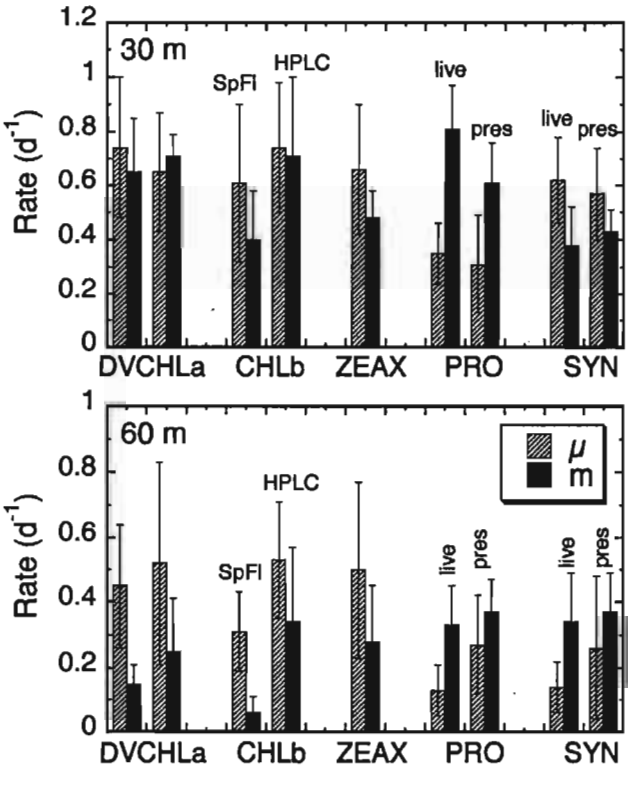

Figure 4. Comparison of mean dilution rate estimates based on flow cytometric (FCM) analyses of prokaryotic picophytoplankton and associated pigments (Table 1). Dv-chl *a* and chl *b* were determined from both spectrofluorometric (SpFl) and HPLC analyses. FCM analyses are for "live" shipboard counts and preserved ("pres") laboratory counts by different machines, procedures, and operators. Vertical line denotes one standard deviation (n = 4 experiments with water from 30 and 60 m).

Table 3. Mean (±Standard Deviation) Instantaneous Rates of Change for Cellular Chlorophyll Fluorescence, Cell Biovolume, and Cellular Pigment Density (Chlorophyll/Biovolume) From FCM-Analyzed Populations During Dilution Incubations[a]

Parameter	30-m Experiments	60-m Experiments
	Prochlorococcus (PRO)	
Fluorescence	0.179 ± 0.080	0.288 ± 0.119
Biovolume	−0.003 ± 0.029	0.002 ± 0.029
Cell Pigment Density	0.182 ± 0.097	0.286 ± 0.131
	Synechococcus (SYN)	
Fluorescence	0.507 ± 0.202	0.481 ± 0.128
Biovolume	0.052 ± 0.031	0.040 ± 0.014
Cell Pigment Density	0.455 ± 0.193	0.441 ± 0.141
	Photosynthetic Eukaryotes (PEUK)	
Fluorescence	0.350 ± 0.124	0.434 ± 0.164
Biovolume	0.182 ± 0.123	0.174 ± 0.116
Cell Pigment Density	0.169 ± 0.079	0.260 ± 0.092

[a]Calculations as described in section 2.6 where chlorophyll is assumed proportional to measured red fluorescence and biovolume varies with $FALS^{0.55}$.

Table 4. Mean rate-Adjusted Estimates of Phytoplankton Growth (μ, d^{-1}) and Microzooplankton Grazing (m, d^{-1}) From EBENE Dilution Experiments[a]

	30 m		60 m	
Parameter	μ, d^{-1}	m, d^{-1}	μ, d^{-1}	m, d^{-1}
Tchl *a*	0.76 (0.29)	0.56 (0.18)	0.27 (0.12)	0.15 (0.09)
mv-chl *a*	0.92 (0.29)	0.52 (0.23)	0.32 (0.08)	0.11 (0.09)
dv-chl *a*	0.52 (0.28)	0.68 (0.11)	0.21 (0.18)	0.20 (0.11)
PRO	0.32 (0.16)	0.61 (0.15)	0.29 (0.15)	0.37 (0.10)
SYN	0.62 (0.16)	0.43 (0.08)	0.30 (0.23)	0.37 (0.12)
PEUK	0.54 (0.18)	0.55 (0.38)	0.44 (0.17)	0.32 (0.11)

[a]Pigment-based rates (Tchl *a*, mv-chl *a*, and dv-chl *a*) are the means from separate spectrofluorometric and HPLC analyses, with growth rates adjusted for net changes in the red chlorophyll fluorescence (cell biovolume)$^{-1}$ as inferred from initial and final sample analyses by flow cytometry (FCM). Abundance-based rates are from FCM analyses of *Prochlorococcus* (PRO), *Synechococcus* (SYN), and photosynthetic eukaryotes (PEUK), with growth rates adjusted for net changes in cellular biovolume as inferred from FCM analyses. Parentheses enclose standard deviations of the means (n = 4). Pigment and abundance-based rates from individual experiments are plotted in Figures 5 and 6, respectively.

in bead-normalized FALS, implying shifts to cells of larger size and damping the net increase in biovolume-specific chlorophyll (Table 3). In contrast, cellular fluorescence changes for PRO apparently occurred independent of size variations, since FALS for these cells varied negligibly between initial and final samples. Size variations for SYN were also low relative to those of PEUKs. Taking both the net changes in cellular fluorescence and size into consideration lowered mean growth rates for Tchl *a*, mv-chl *a* and dv-chl *a* by 0.2 to 0.3 d^{-1} compared to Table 2 estimates (Table 4). For individual experiments as well as the overall means, this decreased substantially the discrepancies between growth and grazing rate estimates from pigment determinations (Figure 6). The effect was particularly notable for the 60-m experiments, where the rate corrections were a larger fraction of the previous raw pigment estimates (e.g., Figure 6 versus Figure 2).

[30] Because of the population differences in cell size increases during the experimental incubations, rate adjustments for biovolume changes were only substantial for eukaryotic phytoplankton, increasing mean growth rates by about 0.2 d^{-1} (Table 4). Since biovolume adjustments did not modify growth rate estimates from PRO cell counts, they continued to show a substantial excess of grazing over growth (Figure 7). In contrast, the adjustments improved the balance between growth and grazing for PEUK, particularly for the 30-m experiments.

3.6. Carbon Production and Grazing Estimates

[31] From the fluorescence- and biovolume-adjusted rates of Figures 5 and 6, we are able to derive two pairs of

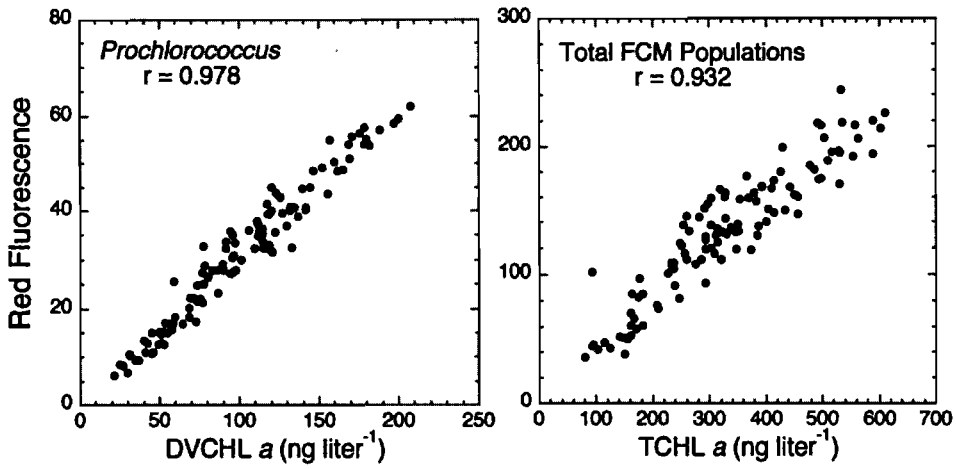

Figure 5. Relationships between FCM estimates of population red fluorescence and HPLC determinations of chl *a*. The data include all initial and final samples from 30- and 60-m dilution experiments. (left) Total red fluorescence for *Prochlorococcus* (total abundance × mean RF/cell) against concentration of divinyl chl *a* and (right) total RF for all FCM-measured populations (sum of abundance × RF/cell for *Prochlorococcus, Synechococcus,* and eukaryotic algae) against measured concentration of total chl *a*. Red fluorescence estimates are FCM measurements normalized to standard beads and divided by 1000; the units are arbitrary.

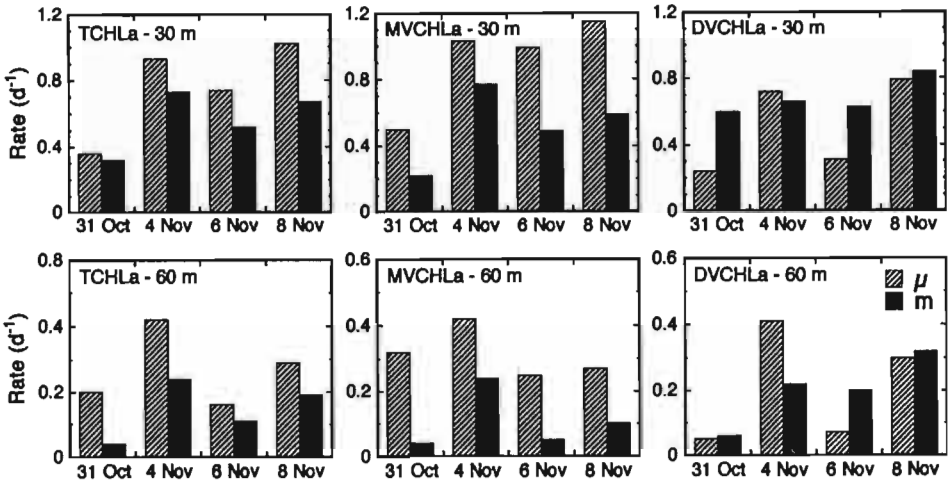

Figure 6. Rates of phytoplankton growth (μ, d^{-1}) and microzooplankton grazing (m, d^{-1}) from analyses based on Tchl *a*, mv-chl *a*, and dv-chl *a*. Rates are averaged for separate spectrofluorometric and HPLC pigment determinations, and growth rates are adjusted for net changes in the red chlorophyll fluorescence (cell biovolume)$^{-1}$ as inferred from initial and final sample analyses by flow cytometry. *X* axis = experiment date. Experiments conducted with water from (top) 30-m depth and (bottom) 60-m depth. Mean rate estimates are in Table 4.

carbon-based estimates for phytoplankton production and protistan grazing. One is from the total community carbon biomass and the community-averaged rates for Tchl *a*; the other is from the sum of production and grazing estimates for each of the component populations (PRO, SYN and PEUK) in FCM analyses. The former yielded production estimates ranging from 8 to 28 mg C m^{-3} d^{-1} at 30 m and 4 to 10 mg C m^{-3} d^{-1} at 60 m (Table 5). In comparison, production estimates for the summed populations averaged 50% lower at 30 m (6–13 mg C m^{-3} d^{-1}) and 50% higher (6–15 mg C m^{-3} d^{-1}) at 60 m.

[32] On the basis of Tchl *a*, protistan grazing accounted for 73% of phytoplankton production at 30 m and 54% at 60 m. From the FCM composite population analyses, protistan grazers consumed an average of 111% of phytoplankton production at 30 m (range = 82–144%) and 82% (range = 70–119%) at 60 m. Community grazing estimates from the sums of the FCM populations were generally consistent with carbon-specific ingestion rates of 100–200% of body mass d^{-1} (Table 6).

4. Discussion

[33] In the present study, we have explored multiparameter analyses of dilution experiments as not only as a means of broadening the taxonomic groups for which we can

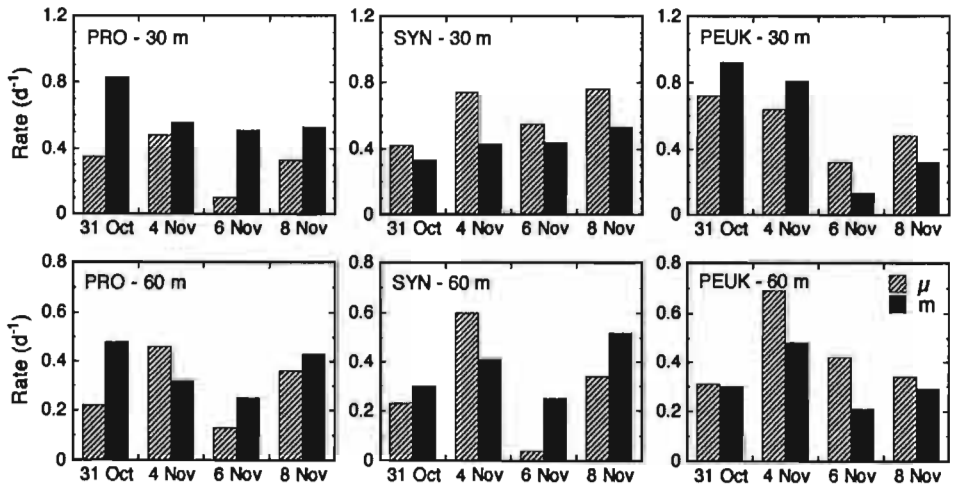

Figure 7. Rates of phytoplankton growth (μ, d^{-1}) and microzooplankton grazing (m, d^{-1}) from cell abundance analyses of *Prochlorococcus* (PRO), *Synechococcus* (SYN), and photosynthetic eukaryotes (PEUK). Rates are adjusted for net changes in cellular biovolumes as inferred from flow cytometric analyses of initial and final samples. *X* axis = experiment date. Experiments conducted with water from (top) 30-m depth and (bottom) 60-m depth. Mean rate estimates are in Table 4.

Table 5. Comparison of Carbon Equivalent Rates of Phytoplankton Production (PP, mg C m^{-3} d^{-1}) and Community Grazing (G, mg C m^{-3} d^{-1}) for Combined Taxa (Sum) and Community Chlorophyll *a* (Total)[a]

		30 m Experiments			60 m Experiments		
Date	Taxon	C_0	PP	G	C_0	PP	G
31 Oct	PRO	7.2	2.0	4.7	4.7	0.9	2.0
	SYN	2.3	1.0	0.8	1.5	0.3	0.4
	PEUK	12.2	8.0	10.2	15.0	5.7	4.5
	sum	21.6	10.9	15.7	21.3	5.9	7.0
	total	21.6	7.9	7.1	21.3	4.6	0.9
4 Nov	PRO	3.3	1.5	1.8	2.8	1.4	1.0
	SYN	0.9	0.8	0.5	0.7	0.5	0.3
	PEUK	18.2	10.7	13.6	17.2	13.2	9.2
	sum	22.5	13.1	15.8	20.7	15.1	10.5
	total	22.5	23.1	18.1	20.7	9.5	5.4
6 Nov	PRO	6.1	0.5	2.5	5.5	0.7	1.3
	SYN	1.4	0.8	0.6	1.2	0.0	0.3
	PEUK	13.9	4.9	2.0	15.1	7.1	3.5
	sum	21.3	6.2	5.2	21.8	7.8	5.1
	total	21.3	17.7	12.4	21.8	3.6	2.5
8 Nov	PRO	6.1	1.8	2.9	4.9	1.7	2.0
	SYN	1.4	1.2	0.8	1.1	0.3	0.5
	PEUK	15.4	8.0	5.3	16.1	5.6	4.8
	sum	22.8	11.0	9.1	22.1	7.7	7.3
	total	22.8	27.9	18.3	22.1	6.7	4.4
	mean sum			10.3	11.4	9.1	7.5
	std. dev			2.9	5.2	4.1	2.2
	mean total			19.1	14.0	6.1	3.3
	std. dev.			8.6	5.4	2.6	2.0

[a] C_0 indicates initial carbon estimates based on FCM and microscopical analyses. Carbon rates are computed from standing stocks and μ'_0 and g specific rates (d^{-1}; Table 4) for *Prochlorococcus* (PRO), *Synechococcus* (SYN), photosynthetic eukaryotes (PEUK), and Tchl *a*.

derive growth and grazing rate estimates, but as an approach to constraining the interpretation of results. Even when based on different pigment measurement techniques (Figures 1 and 4), for example, the good agreement in rate estimates for a given experiment suggests a mean measurement precision of 0.1–0.2 d^{-1}. At the same time, however, the results can be systematically biased by physiological adaptations of the contained phytoplankton assemblage to incubation conditions, no matter how carefully they are designed to reflect the ambient environment. Here we have seen that such biases can be significant (e.g., 0.2–0.3 d^{-1}) with respect to the balance of growth and loss processes, but that complementary analyses by pigment and flow cytometric techniques might be a useful, first-order approach to resolving their effects.

[34] The primary bias identified in the present experiments was an unambiguous increase in the cellular fluorescence of all FCM-distinguishable populations. Thus growth rates based on unadjusted changes of measured chlorophyll consistently overestimated the growth of phytoplankton biomass (biovolume). Photoacclimation would seem to be the most straightforward explanation for cellular fluorescence increase, the implication being that phytoplankton experienced lower light levels in the incubators than at sampled depths in the ambient environment and adjusted their chlorophyll contents accordingly. Consistent with this explanation, we found no differences in the fluorescence increases in bottles incubated with and without added nutrients. On the other hand, deck incubators more typically err on the side of providing more illumination than their calibration ratings because of light penetration through their sidewalls [e.g., *Hiscock et al.*, 2003]. As an alternative therefore it is possible that low-level iron contamination stimulated fluorescence increases in our no-nutrient controls comparable to those in nutrient-amended bottles. As noted in the IronEx II fertilized patch [*Landry et al.*, 2000a, 2000b], phytoplankton chlorophyll adjusts rapidly (hours) at equatorial sea surface temperatures to increased iron availability compared to the lagged response of balanced cell growth (2–3 days). From just initial and final fluorescence measurements in our experiments, we are not able to distinguish light responses from those due to iron. This mechanistic issue therefore remains unresolved. Regardless of mechanism, however, the single cell properties measured by flow cytometry allow one to account for the component of total chlorophyll change due to physiological adjustment in cell chlorophyll content, and thus to determine more accurate estimates of phytoplankton biomass growth. In the sections below, we consider both methodological and ecological interpretations as they pertain to picophytoplankton, production estimates, diatom growth, and the microzooplankton contribution to grazing.

4.1. Dynamics of Picophytoplankton

[35] Picophytoplankton (principally PRO and SYN, but also including small eukaryotic algae) display strong synchronous cycles of cell division and abundance in equatorial waters [e.g., *Vaulot and Marie*, 1999]. Specific growth rates of about one cell division d^{-1} are indicated at optimal light depths, and balanced growth and grazing is implied over 24-hour periods [*Vaulot et al.*, 1995; *André et al.*, 1999; *Vaulot and Marie*, 1999; *Neveux et al.*, 2003]. Indeed, one of the major elements in the explanation of the HNLC condition is a close grazing control of the dominant and competitively superior picophytoplankton, allowing only the larger algae to increase when the limiting resource, iron, becomes more available [e.g., *Price et al.*, 1994; *Landry et al.*, 1997]. Despite general acceptance of this proposition, it has been difficult to demonstrate experimentally. Cell cycle analyses and observed abundance cycles confirm the growth component of the daily cycle but cannot speak to the decline phase, which could be regulated, for example, by viral lysis. At the same time, the dilution technique for assessing growth and grazing rates together has given equivocal results. One of the significant problems has been unreasonably low growth rate estimates for PRO [*Latasa et al.*, 1997; *Landry et al.*, 2000b], which have been ascribed to a

Table 6. Carbon-Specific Ingestion Rates (G/P_o; mgC mgC^{-1} d^{-1}) Based on Microscopical Determinations of the Standing Stock of Heterotrophic Protists (P_o; mg C m^{-3}) and Carbon-Based Estimates of Community Grazing (G, mg C m^{-3} d^{-1}; From Sums, Table 5)

	30 m Experiments			60-m Experiments		
Date	P_o	G	G/P_o	P_o	G	G/P_o
31 Oct	8.8	15.7	1.8	2.3	7.0	3.0
4 Nov	19.0	15.8	0.8	9.9	10.5	1.1
6 Nov	9.8	5.2	0.5	3.3	5.1	1.5
8 Nov	4.3	9.1	2.1	5.2	7.3	1.4
Mean	11.4	1.3		7.5	1.8	
Std. dev.	5.2	0.7		2.2	0.9	

photoadaptive decline of the marker pigment dv-chl *a* due to unusual light sensitivity.

[36] In contrast to previous efforts, the present results show strong experimental support for the grazing control of picophytoplankton. The rate estimates also agree closely with those inferred from the daily oscillations of dv-chl *a* at the equator from fine-scale in situ sampling over the 30–70 m depth range [*Neveux et al.*, 2003]. Of the three 30-m experiments conducted at the equator, adjusted growth (μ'_o) estimates based on dv-chl *a* slightly exceeded grazing mortality (m) in one (0.72 versus 0.66 d^{-1}), μ'_o was slightly <m in another (0.79 versus 0.84 d^{-1}), and μ'_o was substantially <m in the third (0.31 versus 0.63 d^{-1}). Mean μ'_o at 30 m (0.61 d^{-1}), the optimal light depth for PRO growth, was consistent, within day-to-day experimental variability, with the one cell division d^{-1} determined from cell cycle analysis [*Vaulot et al.*, 1995; *Liu et al.*, 1999]. At 60 m, the experimental rate estimates were even more closely balanced (means = 0.26 and 0.25 d^{-1}, respectively) than at 30 m. In comparison, the mean rates from diel dv-chl *a* oscillations in the 30–70 m depth range (μ'_o = 0.40 d^{-1}; m = 0.36 d^{-1}) [*Neveux et al.*, 2003] were intermediate, as one might expect, between experimental rate estimates for the upper and lower portions of this depth range.

[37] In comparing rate estimates for PRO based on dv-chl *a* and FCM cell counts, we note that most of the inconsistencies in experiments conducted with 60-m water can be attributed to the one experiment conducted at 3°S (Figures 5 and 6). For experiments at the equator, the mean rate estimates from FCM counts (0.32 and 0.30 d^{-1} for μ'_o and m, respectively) compare favorably with the 60-m estimates from dv-chl *a* (0.26 and 0.25 d^{-1}). Mean grazing rate estimates from dv-chl *a* and PRO cell counts (0.68 versus 0.61 d^{-1}; Table 4) were also in good agreement for 30-m experiments. Ironically, however, the initial dv-chl *a* growth estimates at 30-m were in close balance with grazing rates (Table 2), and the main effect of the rate *adjustments* was to decrease these pigment-based estimates by 0.1 d^{-1} rather than enhance those from cells counts. Overall, therefore the main discrepancy in experimental rate assessments for *Prochlorococcus* was in 30-m growth rates from FCM cell counts, which were substantially lower than grazing rates at the same depth as well as growth estimates based on pigments. The present results do not offer a definitive explanation for why the cell-based growth estimates differed from the other rate determinations. Nonetheless, because the agreement between μ'_o and m estimates was much better for the 4 November experiment than the others (Figure 7), we speculate that timing differences in the start of these experiments (1300 hours for 4 November; 2200 hours for the other dates) influenced the outcomes. Specifically, the manipulation of seawater samples during the period of synchronized cell division may alter the course of PRO growth and/or cell division during the following day.

[38] In retrospect, low growth rate estimates for *Prochlorococcus* have also been observed for dilution experiments set up in the early morning [e.g., *Landry et al.*, 2000b]. The relatively good pigment-based results here suggest that timing is critical and perhaps that starting experiments in middle to late afternoon, rather than later, might help to minimize the discrepancies between pigment and cell count estimates. This would coincide with the time of maximum water column stratification, ensuring that the cells would be maximally photoadapted to the light depth of collection. More importantly, experiments begun prior to the time of synchronized cell division would effectively capture the true change in cell abundance based on the previous day's growth under ambient conditions, thereby minimizing potential containment artifacts on that rate estimate. Last, for pigment-based assessments, terminating experiments in the declining phase of the daily light cycle would ensure the maximum degradation of pigments ingested by protistan consumers [e.g., *Klein et al.*, 1986; *Strom*, 1993].

4.2. Phytoplankton Community Growth and Production

[39] The adjusted community estimates of phytoplankton growth from the present study (Tchl *a* mean = 0.76 d^{-1} at 30-m) are comparable to previous results from HNLC equatorial surface waters [*Landry et al.*, 1995a, 1995b, 2000b; *Verity et al.*, 1996; *Latasa et al.*, 1997]. However, the range is broad, and higher raw pigment estimates (Table 2) fit previous results equally well. We thus examine ^{14}C production estimates from the EBENE cruise as an independent constraint against which we can evaluate the reasonableness of our results and interpretations.

[40] For approximately similar circumstances to those of the present study, *Laws et al.* [2000] determined that measured rates of ^{14}C uptake would be expected to equal about 80% of true carbon growth of phytoplankton due to losses to grazers and microbial respiration during incubation. By this criterion, the highest calculated production in the present study (27.9 mg C m^{-3} d^{-1}; Table 5) is a good match with the highest measured rate of ^{14}C uptake on the EBENE cruise (22.8 mg C m^{-3} d^{-1}) [*Le Bouteiller et al.*, 2003]. *Le Bouteiller et al.* [2003] also determined a mean Productivity Index (PI = carbon fixation normalized to initial Tchl *a*) of 66 mg C mg chl a^{-1} d^{-1} for the daily photocycle, from which we can compute an expected ^{14}C uptake rate based on the initial Tchl *a* of 30-m dilution experiments (Table 2). This computed rate, 18.4 mgC m^{-3} d^{-1}, is slightly less than the production mean based on Tchl *a* estimates of phytoplankton growth and grazing (19.1 mgC m^{-3} d^{-1}; Table 5), and 80% of the average rate for the three experiments at the equator (22.9 mgC m^{-3} d^{-1}). In contrast, the unadjusted rates for Tchl *a* would lead to production estimates exceeding ^{14}C measurements by >50%. The more favorable comparisons with our adjusted rate estimates do not prove that these rates are completely accurate. They do, however, demonstrate that the combination of carbon standing stocks and rates from the present analyses provide carbon production estimates in very good agreement with constraints of independent assessments based on the established method for measuring primary production.

4.3. Diatom Growth and Silica Cycling

[41] Diatoms are the phytoplankton group most associated with iron-limited growth rates in HNLC systems [e.g., *Morel et al.*, 1991]. Paradoxically, several studies similar to the present one have shown very high growth rate estimates for diatoms, at least as can be inferred from the pigment fucoxanthin (FUCO) [e.g., *Strom and Welschmeyer*, 1991; *Latasa et al.*, 1997; *Landry et al.*, 2000b]. One explanation

is that the tiny (7–10 μm) pennate cells that dominate open ocean diatom assemblages might be uniquely adapted for high growth under low iron conditions, while larger forms are more strongly iron-limited [*Landry et al.*, 2000b]. In the present study, this explanation appears to be at odds with diatom growth rate inferences, from the same cruise and stations, based on silicate uptake [*Leynaert et al.*, 2001]. According to *Leynaert et al* [2001], the specific growth rates of diatoms averaged 0.35 d^{-1} in equatorial surface waters, about fivefold lower than FUCO-based assessments (Table 2).

[42] Since Si estimates of diatom growth are computed by dividing Si uptake rates by biogenic silica (BSi) standing stocks, these rates will be low if a substantial fraction of the BSi is not associated with living cells. According to *Brzezinski* [1985], the mean molar C:Si ratio of diatoms in the oceans is 7.7, but this can decrease by about threefold (i.e., to 2.5) under severely iron deficient conditions [*Takeda*, 1998]. In the present experiments, the mean microscopical estimate of diatom-associated carbon for 30-m samples at the equator (540 ng C L^{-1} = 45 nmol C L^{-1}) was about 1.3 times the molar concentration of BSi at the same station and depth [*Leynaert et al.*, 2001]. Even allowing for uncertainties in the assessment of living diatom biomass and other organisms (e.g., radiolarians and silicaflagellates) with silica tests, the implied C:Si ratio of 1.3 is too low to be explained only by living cells. A substantial "nonliving" pool of BSi must therefore exist, perhaps as grazer produced fragments of frustrules in various stages of dissolution. This scenario would be consistent with the high rates of Si remineralization suggested for equatorial surface waters [*Blain et al.*, 1999; *Landry et al.*, 2000b].

[43] If diatom production contributes substantially to carbon export in the equatorial Pacific [*Leynaert et al.*, 2001], this must be in addition to their grazing losses to microzooplankton and mesozooplankton. The present grazing rate estimate for diatoms (0.56 d^{-1} at the equator) therefore sets a conservative lower limit to the growth rate that diatoms must achieve to remain at steady state with no contribution to export. With this mean grazing rate and the other information at hand for 30-m experiments at the equator, diatom carbon biomass (C_{diat} = 45 nmol C L^{-1}), Si-uptake rate (SiUp = 27 nmol L^{-1} d^{-1}), and an intermediate C:Si ratio of 5.0, we can compute a diatom growth rate that satisfies all constraints. The production equation in Section 2.6, SiUp * $C:Si/C_{diat}$ = 3.0 = μ * ($e^{\mu-0.56}$ − 1)/(μ-0.56), is solved with a growth rate (μ) of 1.6 d^{-1}. The new estimate is about 20% lower than the initial 30-m rate determination for FUCO at the equator (1.97 d^{-1}), or about the same proportional decrease as the fluorescence correction for mv-chl *a* (Table 4). By similar calculation, the 30-m estimates of Si uptake (3.8 nmol L^{-1} d^{-1}), diatom biomass (10 nmol C L^{-1}), and microzooplankton grazing (0.31 d^{-1}) at 3°S imply diatom growth rates of 1.2 d^{-1}, a decline of about 30% compared to the growth estimate (1.7 d^{-1}) based on FUCO. For experiments at 60 m, however, growth rate estimates from the Si uptake calculations (0.9–1.0 d^{-1}) were not less than the initial FUCO-based determinations at either the equator or 3°S.

[44] From the above calculations, we can see that the Si uptake rates of *Leynaert et al.* [2001] are quite compatible with the present results and help to constrain the growth rates derived from pigments. The combination of data suggests a relatively small biomass of diatoms, comprising as little as 30–40% of the particulate biogenic silica, but turning over at a rapid rate. If a large portion of this diatom production escapes grazing by microzooplankton, as it indeed appears to do in our experiments, steady state concentrations must be maintained by a combination of other losses, including sinking, grazing by larger consumers (mesozooplankton) or advective transport. The latter has been shown to be important in the central Pacific, leading to higher phytoplankton biomass several degrees north and south of the equator [*Landry et al.*, 1997] and dense aggregations of buoyant diatoms at convergent fronts [*Yoder et al.*, 1994]. That such features were not evident in the present study may reflect the influence of a passing instability wave [*Eldin and Rodier*, 2003; *Neveux et al.*, 2003].

[45] The nonspecific grazing of mesozooplankton, as measured by gut fluorescence, was sufficient during EBENE to account for the portion of phytoplankton production not consumed by microzooplankton, including that produced by diatoms [*Le Borgne and Landry*, 2003]. Nonetheless, it is difficult to imagine how this relatively sparse assemblage could effectively clear the euphotic zone at rates of 1 d^{-1}. Overall, diatom concentrations were so low in the present experiments that relatively large errors in their rate assessments (e.g., different rates of photoacclimation or iron response of FUCO relative to mv-chl *a*) would have had negligible effects on the estimates of total community production and grazing. Given the importance of diatoms in equatorial bloom dynamics, however, a more precise accounting needs to be done of the diatom production and its alternate fates under ambient low iron conditions.

4.4. Protist Contribution to the Grazing Balance

[46] With respect to the EBENE goal of quantifying grazer contributions to HNLC phytoplankton control, the present experiments indicate that microzooplankton consumed an average of 69% of phytoplankton production (Table 5; mean Tchl *a* estimates of G and PP from all experiments). Lower estimates of microzooplankton grazing, about 50% of production, were reported for EqPac cruise TTO11 (August–September 1992) during normal upwelling conditions [*Landry et al.*, 1995a; *Latasa et al.*, 1997] and in the ambient environment during IronEx II [*Landry et al.*, 2000b]. These estimates were uncorrected for changes in cellular chlorophyll content, and consequently may have been understated. During the El Niño phase of the EqPac studies, however, microzooplanton grazing accounted for >80% of uncorrected phytoplankton production [*Landry et al.*, 1995a, 1997; *Latasa et al.*, 1997; *Verity et al.*, 1996].

[47] One of the differences between El Niño and normal upwelling conditions in the EqPac study was the advective transport of net phytoplankton growth away from the equator during the upwelling phase [*Landry et al.*, 1997]. Net phytoplankton growth measured by instrumented drifters amounted to almost 0.2 d^{-1}, the difference between 30-m growth and grazing estimates for the phytoplankton community in the present study. Here it appears that grazing by mesozooplankton accounted for most of the difference between our growth and grazing estimates [*Champalbert et al.*, 2003; *Le Borgne and Landry*, 2003], leaving little of phytoplankton production unexplained by grazing losses.

[48] Although we have focused on unraveling phytoplankton physiological adaptations that may have influenced growth rate estimates, it is also possible that microzooplankton grazing rates may have been underestimated to some extent if dark conditions during the last few hours of the dilution incubations left some fraction of the grazed pigment undegraded [e.g., *Klein et al.*, 1986; *Strom*, 1993; *Strom et al.*, 1998]. In this regard, we note some support for light-mediated degradation of grazed pigment in the comparison of pigment and FCM results at the 60-m light level (Table 4). However, the relatively good agreement between mean grazing rates from pigment and FCM analyses in 30-m experiments indicates that this effect was small, if any, for light levels more representative of the upper euphotic zone.

[49] In summary, the present results provide good experimental evidence for grazer regulation of picophytoplankton populations in the HNLC equatorial Pacific, and rate estimates are in good agreement with the daily cycle of growth and grazing inferred from *in situ* fluctuations in the 30–70 m depth range. The data are also consistent with phytoplankton community production estimates from ^{14}C-bicarbonate uptake and with ^{32}Si-silicate uptake rates by diatoms. Grazing by microzooplankton accounted for the majority (69%) of equatorial phytoplankton production during the EBENE cruise, consistent with the smaller grazing contribution determined in contemporaneous studies of mesozooplankton.

[50] **Acknowledgments.** This study was supported in part by NSF grants OCE-9218152, -9617409 and -9911765 as well as travel and logistical support from the IRD Centre de Noumea. We gratefully acknowledge the many shipmates and colleagues who facilitated and contributed to our efforts, particularly Chief Scientist, R. Le Borgne, and the captain and crew of the N.O. *L'Atalante*. This paper is contribution 980 from the U.S. JGOFS Program and 6242 from the School of Ocean and Earth Science and Technology, University of Hawaii at Manoa, Honolulu, USA.

References

Andersen, R. A., D. Potter, R. R. Bidigare, M. Latasa, K. Rowan, and C. J. O'Kelly, Characterization and phylogenetic position of the enigmatic golden alga *Phaeothamnion confervicola*: Ultrastructure, pigment composition and partial SSU rDNA sequence, *J. Phycol.*, *34*, 286–298, 1998.

André, J. M., C. Navarette, J. Blanchot, and M.-H. Radenac, Picophytoplankton dynamics in the equatorial Pacific: Growth and grazing rates from cytometric counts, *J. Geophys. Res.*, *104*, 3369–3380, 1999.

Bidigare, R. R., Analysis of algal chlorophylls and carotenoids, in *Marine Particles: Analysis and Characterization*, *Geophys. Monogr. Ser.*, vol. 63, edited by D. C. Hurd and D. W. Spencer, pp. 119–123, AGU, Washington, D.C., 1991.

Bidigare, R. R., and M. E. Ondrusek, Spatial and temporal variability of phytoplankton pigment distributions in the central equatorial Pacific Ocean, *Deep Sea Res., Part II*, *43*, 809–833, 1996.

Binder, B. J., S. W. Chisholm, R. J. Olson, S. L. Frankel, and A. Z. Worden, Dynamics of picophytoplankton, ultraphytoplankton and bacteria in the central equatorial Pacific, *Deep Sea Res., Part II*, *43*, 907–931, 1996.

Blain, S., P. Treguer, and M. Rodier, Stocks and fluxes of biogenic silica in the western oligotrophic equatorial Pacific, *J. Geophys. Res.*, *104*, 3357–3368, 1999.

Blanchot, J., and M. Rodier, Picophytoplankton abundance and biomass in the western tropical Pacific Ocean during the 1992 El Niño year: Results from flow cytometry, *Deep Sea Res., Part I*, *43*, 877–895, 1996.

Brown, S. L., M. R. Landry, J. Neveux, and C. Dupouy, Microbial community abundance and biomass along a 180° transect in the equatorial Pacific during an El Niño-Southern Oscillation cold phase, *J. Geophys. Res.*, *108*(C12), 8139, doi:10.1029/2001JC000817, in press, 2003.

Brzezinski, M. A., The Si:C ratio of marine diatoms: Interspecific variability and the effect of some environmental variables, *J. Phycol.*, *21*, 347–357, 1985.

Burkill, P. H., E. S. Edwards, A. W. S. John, and M. A. Sleigh, Microzooplankton and their herbivorous activity in the northeastern Atlantic Ocean, *Deep Sea Res., Part II*, *40*, 479–493, 1993.

Calbet, A., and M. R. Landry, Mesozooplankton influences on the microbial food web: Direct and indirect trophic interactions in the oligotrohic open-ocean, *Limnol. Oceanogr.*, *44*, 1370–1380, 1999.

Champalbert, G., J. Neveux, R. Gaudy, and R. Le Borgne, Diel variations of copepod feeding and grazing impact in the high-nutrient, low-chlorophyll zone of the equatorial Pacific Ocean (0°; 3°S, 180°), *J. Geophys. Res.*, *108*(C12), 8145, doi:10.1029/2001JC000810, in press, 2003.

Coale, K. H., et al., A massive phytoplankton bloom induced by an ecosystem scale iron fertilization experiment in the equatorial Pacific Ocean, *Nature*, *383*, 495–501, 1996.

Cullen, J. J., M. R. Lewis, C. O. Davis, and R. T. Barber, Photosynthetic characteristics and estimated growth rates indicate grazing is the proximate control of primary production in the equatorial Pacific, *J. Geophys. Res.*, *97*, 639–654, 1992.

DuRand, M. D., Phytoplankton growth and diel variations in beam attenuation through individual cell analysis, Ph.D. diss., 267 pp., Mass. Inst. of Technol./Woods Hole Oceanogr. Inst., Woods Hole, Mass., 1995.

DuRand, M. D., and R. J. Olson, Contributions of phytoplankton light scattering and cell concentration changes to diel variations in beam attenuation in the equatorial Pacific from flow cytometric measurements of pico-, ultra- and nanoplankton, *Deep Sea Res., Part II*, *43*, 891–906, 1996.

Eldin, G., and M. Rodier, Ocean physics and nutrient fields along 180° during an El Niño-Southern Oscillation cold phase, *J. Geophys. Res.*, *108*(C12), 8137, doi:10.1029/2000JC000746, in press, 2003.

Eppley, R. W., F. M. H. Reid, and J. D. H. Strickland, Estimates of phytoplankton crop size, growth rate, and primary production, in *The Ecology of the Plankton off La Jolla California in the Period April Through September, 1967*, edited by J. D. H. Strickland, *Bull. Scripps Inst. Oceanogr.*, *17*, 33–42, 1970.

Fitzwater, S. E., G. A. Knauer, and J. H. Martin, Metal contamination and its effect on primary production measurements, *Limnol. Oceanogr.*, *27*, 544–551, 1982.

Frost, B. W., and N. C. Franzen, Grazing and iron limitation in the control of phytoplankton stock and nutrient concentration: A chemostat analogue of the Pacific equatorial upwelling zone, *Mar. Ecol. Prog. Ser.*, *83*, 291–303, 1992.

Garrison, D. L., et al., Microbial food web structure in the Arabian Sea: A JGOFS study, U.S., *Deep Sea Res., Part II*, *47*, 1387–1422, 2000.

Hiscock, M. R., J. Marra, W. O. Smith Jr., R. Goericke, C. I. Measures, S. Vink, R. J. Olson, H. M. Sosik, and R. T. Barber, Primary productivity and its regulation in the Pacific sector of the Southern Ocean, *Deep Sea Res., Part II*, *50*, 533–558, 2003.

Jeffrey, S. W., and M. Vesk, Introduction to marine phytoplankton and their pigment signatures, *Phytoplankton Pigments in Oceanography: Guidelines to Modern Methods*, edited by S. W. Jeffrey, R. C. F. Mantoura, and S. W. Wright, pp. 37–82, UNESCO Publ., Paris, 1997.

Klein, B., W. W. C. Gieskes, and G. C. Kraay, Digestion of chlorophylls and carotenoids by the marine protozoan Oxyrrhis marina studied by h.p.l.c. analysis of algal pigments, *J. Plankton Res.*, *8*, 827–836, 1986.

Landry, M. R., Estimating rates of growth and grazing of phytoplankton by dilution, in *Handbook of Methods in Aquatic Microbial Ecology*, edited by P. K. Kemp et al., pp. 715–722, CRC Press, Boca Raton, Fla., 1993.

Landry, M. R., and R. P. Hassett, Estimating the grazing impact of marine micro-zooplankton, *Mar. Biol.*, *67*, 283–288, 1982.

Landry, M. R., and D. L. Kirchman, Microbial community structure and variability in the tropical Pacific, *Deep Sea Res., Part II*, *49*, 2669–2693, 2002.

Landry, M. R., J. Constantinou, and J. Kirshtein, Microzooplankton grazing in the central equatorial Pacific during February and August, 1992, *Deep Sea Res., Part II*, *42*, 657–671, 1995a.

Landry, M. R., J. Kirshtein, and J. Constantinou, A refined dilution technique for measuring the community grazing impact of microzooplankton, with experimental tests in the central equatorial Pacific, *Mar. Ecol. Prog. Ser.*, *120*, 53–63, 1995b.

Landry, M. R., et al., Iron and grazing constraints on primary production in the central equatorial Pacific: An EqPac synthesis, *Limnol. Oceanogr.*, *42*, 405–418, 1997.

Landry, M. R., S. L. Brown, L. Campbell, J. Constantinou, and H. Liu, Spatial patterns in phytoplankton growth and microzooplankton grazing in the Arabian Sea during monsoon forcing, *Deep Sea Res., Part II*, *45*, 2353–2368, 1998.

Landry, M. R., M. E. Ondrusek, S. J. Tanner, S. L. Brown, J. Constantinou, R. R. Bidigare, K. H. Coale, and S. Fitzwater, Biological response to iron fertilization in the eastern equatorial Pacific (IronEx II). I. Microplankton community abundances and biomass, *Mar. Ecol. Prog. Ser.*, *201*, 27–42, 2000a.

Landry, M. R., J. Constantinou, M. Latasa, S. L. Brown, R. R. Bidigare, and M. E. Ondrusek, Biological response to iron fertilization in the eastern equatorial Pacific (IronEx II). III. Dynamics of phytoplankton growth and microzooplankton grazing, *Mar. Ecol. Prog. Ser.*, *201*, 57–72, 2000b.

Latasa, M., and R. R. Bidigare, A comparison of phytoplankton populations of the Arabian Sea during the spring intermonsoon and southwest monsoon of 1995 as described by HPLC-analyzed pigments, *Deep Sea Res., Part II*, *45*, 2133–2170, 1998.

Latasa, M., R. R. Bidigare, M. E. Ondrusek, and M. C. Kennicutt II, HPLC analysis of algal pigments: A comparison exercise among laboratories and recommendations for improved analytical performance, *Mar. Chem.*, *51*, 3115–3124, 1996.

Latasa, M., M. R. Landry, L. Schlüter, and R. R. Bidigare, Pigment-specific growth and grazing rates of phytoplankton in the central equatorial Pacific, *Limnol. Oceanogr.*, *42*, 289–298, 1997.

Laws, E. A., M. R. Landry, R. T. Barber, L. Campbell, M.-L. Dickson, and J. Marra, Carbon cycling in primary production bottle incubations: Inferences from grazing experiments and photosynthetic studies using 14C and 18O in the Arabian Sea, *Deep Sea Res., Part II*, *47*, 1339–1352, 2000.

Le Borgne, R., and M. R. Landry, EBENE: A JGOFS investigation of plankton variability and trophic interactions in the equatorial Pacific (180°), *J. Geophys. Res.*, *108*(C12), 8136, doi:10.1029/2001JC001252, in press, 2003.

Le Bouteiller, A., J. Blanchot, and J. Neveux, Primary production, new production, and growth rate in the equatorial Pacific: Changes from mesotrophic to oligotrophic regime, *J. Geophys. Res.*, *108*(C12), 8141, doi:10.1029/2000JC000914, in press, 2003.

Leynaert, A., P. Treguer, C. Lancelot, and M. Rodier, Silicon limitation of biogenic silica production in the equatorial Pacific, *Deep Sea Res., Part I*, *48*, 639–660, 2001.

Liu, H., M. R. Landry, D. Vaulot, and L. Campbell, Prochlorococcus growth rates in the central equatorial Pacific: An application of the f_{max} approach, *J. Geophys. Res.*, *104*, 3391–3392, 1999.

Miller, C. B., B. W. Frost, P. A. Wheeler, M. R. Landry, N. Welschmeyer, and T. M. Powell, Ecological dynamics in the subarctic Pacific, a possibly iron-limited ecosystem, *Limnol. Oceanogr.*, *36*, 1600–1615, 1991.

Monger, B. C., and M. R. Landry, Flow cytometric analysis of marine bacteria using Hoechst 33342, *Appl. Environ. Microbiol.*, *59*, 905–911, 1993.

Morel, A., Optics of marine particles and marine optics, *Particle Analysis in Oceanography, NATO ASI Ser., Ser. G*, vol. 27, edited by S. Demers, pp. 144–188, Springer-Verlag, New York, 1991.

Morel, F. M., J. G. Rueter, and N. M. Price, Iron nutrition of phytoplankton and its possible importance in the ecology of open ocean regions with high nutrient and low biomass, *Oceanography*, *4*, 56–61, 1991.

Neveux, J., and F. Lantoine, Spectrofluorometric assay of chlorophylls and phaeopigments using the least squares approximation technique, *Deep Sea Res., Part A*, *40*, 1747–1765, 1993.

Neveux, J., C. Dupouy, J. Blanchot, A. Le Bouteiller, M. R. Landry, and S. L. Brown, Diel dynamics of chlorophylls in high-nutrient, low-chlorophyll waters of the equatorial Pacific (180°): Interactions of growth, grazing, physiological responses, and mixing, *J. Geophys. Res.*, *108*(C12), 8140, doi:10.1029/2000JC000747, in press, 2003.

Pitchford, J. W., and J. Brindley, Iron limitation, grazing pressure and high nutrient-low chlorophyll (HNLC) regions, *J. Plankton Res.*, *21*, 525–547, 1999.

Price, N. M., B. A. Ahner, and F. M. M. Morel, The equatorial Pacific Ocean: Grazer-controlled phytoplankton populations in an iron-limited ecosystem, *Limnol. Oceanogr.*, *39*, 520–534, 1994.

Shalapyonok, A., R. J. Olson, and L. S. Shalapyonok, Arabian Sea phytoplankton during southwest and northeast monsoons 1995: Composition, size structure and biomass from individual cell properties measured by flow cytometry, *Deep Sea Res., Part II*, *48*, 1231–1261, 2001.

Sherr, B. F., E. B. Sherr, and R. D. Fallon, Use of monodispersed, fluorescently-labeled bacteria to estimate in situ protozoan bacterivory, *Appl. Environ. Microbiol.*, *53*, 958–965, 1987.

Sherr, E. B., and B. F. Sherr, Preservation and storage of samples for enumeration of heterotrophic protists, in *Handbook of Methods in Aquatic Microbial Ecology*, edited by P. K. Kemp et al., pp. 207–212, CRC Press, Boca Raton, Fla., 1993.

Strathmann, R. R., Estimating the organic carbon content of phytoplankton from cell volume or plasma volume, *Limnol. Oceanogr.*, *12*, 411–418, 1967.

Strom, S. L., Production of phaeopigments by marine protozoa: Results of laboratory experiments analyzed by HPLC, *Deep Sea Res., Part I*, *40*, 57–80, 1993.

Strom, S. L., and N. A. Welschmeyer, Pigment-specific rates of phytoplankton growth and microzooplankton grazing in the open subarctic Pacific Ocean, *Limnol Oceanogr.*, *36*, 50–63, 1991.

Strom, S. L., T. A. Morello, and K. J. Bright, Protozoan size influences algal pigment degradation during grazing, *Mar. Ecol. Prog. Ser.*, *164*, 189–197, 1998.

Takeda, S., Influence of iron availability on nutrient consumption ratio of diatoms in oceanic waters, *Nature*, *393*, 744–777, 1998.

Vaulot, D., CYTOPC: Processing software for flow cytometric data, *Signal Noise*, *2*, 8, 1989.

Vaulot, D., and D. Marie, Diel variability of photosynthetic picoplankton in the equatorial Pacific, *J. Geophys. Res.*, *104*, 3297–3310, 1999.

Vaulot, D., D. Marie, R. J. Olson, and S. W. Chisholm, Growth of Prochlorococcus, a photosynthetic prokaryote, in the equatorial Pacific Ocean, *Science*, *268*, 1480–1482, 1995.

Verity, P. G., D. K. Stoecker, M. E. Sieracki, and J. R. Nelson, Grazing, growth and mortality of microzooplankton during the 1989 North Atlantic spring bloom at 47°N, 18°W, *Deep Sea Res., Part II*, *40*, 1793–1814, 1993.

Verity, P. G., D. K. Stoecker, M. E. Sieracki, and J. R. Nelson, Microzooplankton grazing of primary production at 140°W in the equatorial Pacific, *Deep Sea Res., Part II*, *43*, 1227–1255, 1996.

Wright, S. W., S. W. Jeffrey, R. F. C. Mantoura, C. A. Llewellyn, T. Bjornland, D. Repeta, and N. Welschmeyer, Improved HPLC method for the analysis of chlorophylls and carotenoids from marine phytoplankton, *Mar. Ecol. Prog. Ser.*, *77*, 183–196, 1991.

Yoder, J. A., S. G. Ackelson, R. T. Barber, P. Flament, and W. M. Balch, A line in the sea, *Nature*, *371*, 689–692, 1994.

R. R. Bidigare, S. L. Brown, S. Christensen, and M. R. Landry, Department of Oceanography, University of Hawaii at Manoa, 1000 Pope Rd., Honolulu, HI 96822, USA. (landry@soest.hawaii.edu)

J. Blanchot, Station Biologique de Roscoff, IRD, BP 74, 29682 Roscoff cedex, France.

C. Dupouy, LODYC (CNRS-IRD-UPMC), UMR 7617, UPMC, 4 Place Jussieu, 75452 Paris, France.

J. Neveux, Observatoire Océanologique de Banyuls (CNRS-UPMC), Laboratoire Arago (UMR 7621), BP44, 66651 Banyuls sur Mer, France.

Landry M.R., Brown S.L., Neveux J., Dupouy Cécile, Blanchot Jean, Christensen S., Bidigare R.R. (2003)

Phytoplankton growth and microzooplankton grazing in high-nutrient, low-chlorophyll waters of the equatorial

Pacific : community and taxon-specific rate assessments from pigment and flow cytometric analyses

In: A JGOFS investigation of plankton variability and trophic interactions in the central equatorial Pacific (EBENE)

Journal of Geophysical Reasearch, 108 (C12), 7-1 - 7-14

ISSN 0148-0227